A simple high-throughput approach to identify actionable drug responses in patient-derived tumor organoids

Nhan Phan[1,‡], Jenny J. Hong[1], Bobby Tofig[2], Matthew Mapua[1], Jin Huang[3], Sanaz Memarzadeh[3-7], Robert Damoiseaux[3,8] and Alice Soragni[1,7]*

[1]Division of Hematology-Oncology, Department of Medicine, David Geffen School of Medicine, University of California Los Angeles, CA, 90095
[2]Molecular Screening Shared Resource, California NanoSystems Institute, University of California Los Angeles, CA 90095
[3]Department of Obstetrics and Gynecology, David Geffen School of Medicine, University of California Los Angeles, CA, 90095
[4]Eli and Edythe Broad Center of Regenerative Medicine and Stem Cell Research, University of California Los Angeles, CA 90095
[5]The VA Greater Los Angeles Health Care System, Los Angeles, CA, 90073
[6]Department of Biological Chemistry, University of California Los Angeles, CA 90095
[7]Molecular Biology Institute, University of California Los Angeles, CA 90095
[8]Department of Molecular and Medicinal Pharmacology, David Geffen School of Medicine, University of California Los Angeles, CA, 90095
‡Present address: Laboratory of Stem Cell Research and Application, University of Science, Vietnam National University, HCM City, Vietnam

*Correspondence to AS (alices@mednet.ucla.edu)

Abstract

There is increasing interest in developing 3D tumor organoid models for drug development and personalized medicine applications. While tumor organoids are in principle amenable to high-throughput drug screenings, progress has been hampered by technical constraints and extensive manipulations required by current methodologies. Here, we introduce a miniaturized, fully automatable, flexible high-throughput method using a simplified geometry to rapidly establish 3D organoids from cell lines and primary tissue and robustly assay drug responses.

Introduction

Cancer therapy is rapidly progressing toward individualized regimens not based on the organ of origin, but rather on the molecular characteristics of tumors. Next generation sequencing (NGS) is typically regarded as the key to access this potentially actionable molecular information[1,2]. However, recent studies showed how only a small number of cancers can be singled out and targeted with this approach, in part because very few gene alteration-drug pairs are unequivocally established[3–7]. Thus, functional precision therapy approaches where the primary tumor tissue is directly exposed to drugs to determine which may be efficacious have the potential to boost personalized medicine efforts and influence clinical decisions[4,8]. Establishing patient-derived xenografts (PDX) is a costly and time consuming option that only allows to screen very few potential drugs. Conversely, ex vivo 3D tumor spheroids or organoids derived from primary cancers can be easily established and potentially scaled to screen hundreds to thousands of different conditions.

3D cancer models have been consistently shown to faithfully recapitulate features of the tumor of origin in terms of cell differentiation, heterogeneity, histoarchitecture and clinical drug response[4,9–16]. Various methods to set up tumor spheroids or organoids have been proposed, including using low-attachment U-bottom plates, feeding layers or various biological and artificial matrices[10,13,14,17–23]. Methods using low-attachment U-bottom plates ideally only carry one organoid per well, have limited automation and final assay capabilities[19–21]. In addition, not all cells are capable of forming organized 3D structures with this method. Approaches that include a bio-matrix, such as Matrigel, have the potential to offer a scalable alternative in which cancer cells thrive[10,15,24,25]. However, most approaches so far rely on thick volumes of matrix which is not cost-effective, potentially hard for drugs to efficiently penetrate and difficult to dissolve fully at the end of the experiment[24]. In other applications, organoids are first formed and then transferred to different plates for drug treatment or final readout which can result in the tumor spheres sticking to plastic or breaking[15,25]. In addition, some assays require to disrupt the organoids to single cell suspensions at the end of the experiment[17,23]. All of these manipulations introduce significant variability limiting applicability in screening efforts[13].

To overcome these limitations, we introduce a facile assay system to screen 3D tumor organoids that takes advantage of a specific geometry. Our miniaturized ring methodology does not require functionalized plates. Organoids are assayed in the same plate where they are seeded, with no need for sample transfer at any stage or dissociation of the pre-formed tumor organoids to single cell suspensions. Here, we show that the mini-ring approach is simple, robust, requires few cells and can be easily automated for high-throughput applications. Using this method, we were able to rapidly identify clinically actionable drug sensitivities for several primary ovarian cancer and high-grade serous tumors.

Results and Discussion

Mini-ring setup and assays optimization

In order to rapidly screen organoids, we first established a miniaturized system that allows to setup hundreds of wells and perform assays with minimal manipulation. We adapted the geometry used to plate tumor cells in Matrigel to generate mini-rings around the rim of the wells. This is attained by plating single cell suspensions obtained from a cell line or a surgical specimen pre-mixed with cold Matrigel (3:4 ratio) in a ring shape around the rim in 96 well plates (Fig. 1a). The combination of small volume plated (10 μl) and surface tension holds the cells in place until the Matrigel solidifies upon incubation at 37°C and prevents 2D growth at the center of the wells. This configuration allows for media addition and removal so that changes of conditions or treatment addition to be easily performed by pipetting directly in the center of the well, preventing any disruption of the gel. Cancer cell lines grown in mini-ring format give rise to organized tumor organoids that recapitulate features of the original histology (Fig 1b and S1; Table S1). Similarly, we can routinely establish patient-derived tumor organoids (PDTOs) using the same geometry. Primary patient samples grow and maintain the heterogeneity of the original tumor as expected (Fig. 1b).

Next, we optimized treatment protocols and readouts for the mini-ring approach. Our standardized paradigm includes: seeding cells on day 0, establishing organoids for 2-3 days followed by two consecutive daily drug treatments, each performed by complete medium change (Fig. 1c). As an example, small scale screenings were performed using three drugs at five different concentrations in triplicates, ReACp5, Staurosporine and Doxorubicin (Fig. 1d-g). We optimized different readouts in order to adapt the method to a specific research question or instrument availability. After seeding cells in standard white plates, we performed a lumines-

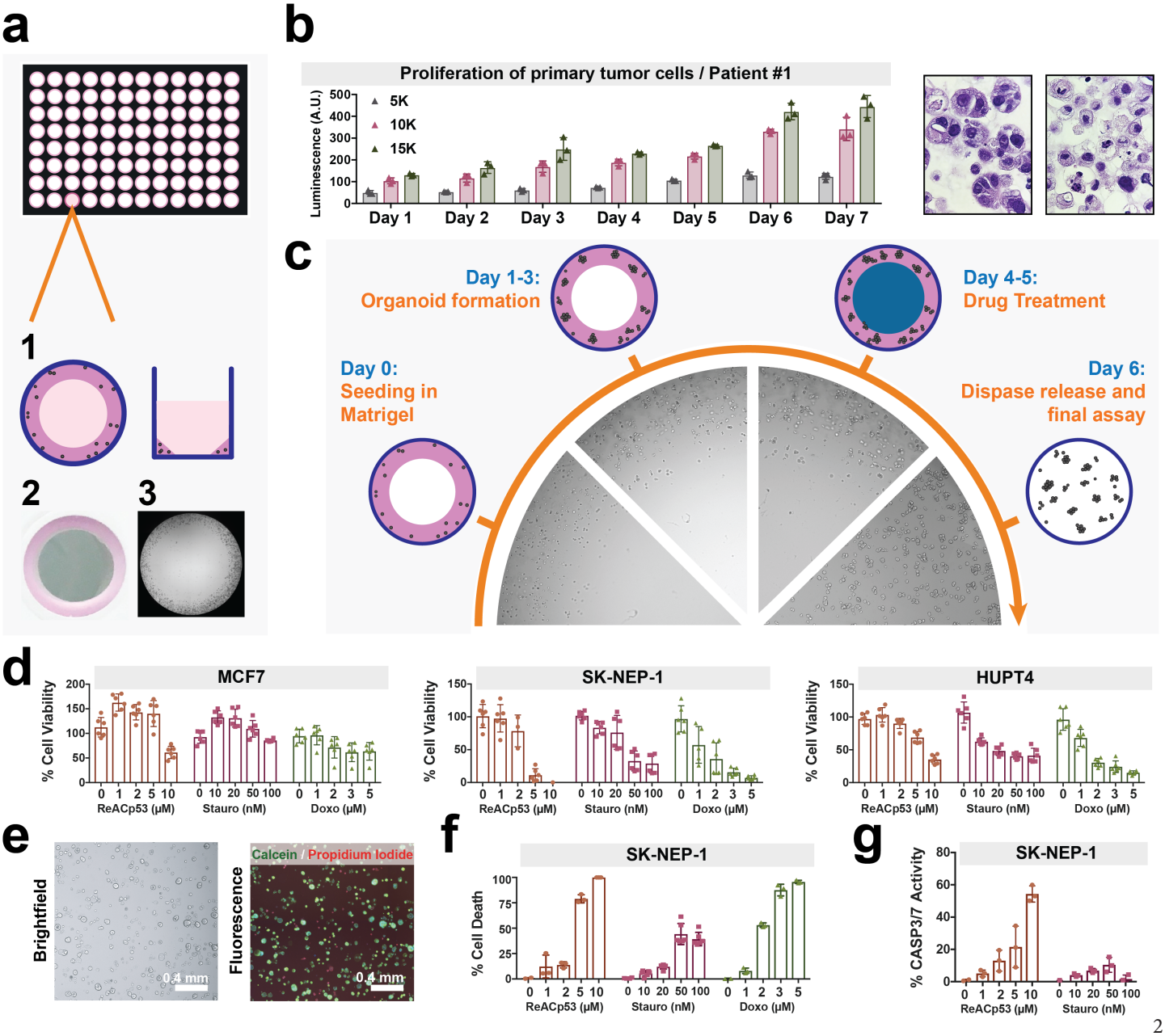

Figure 1. The mini-ring method for 3D tumor cell biology. (a) Schematics of the mini-ring setup. Cells are plated in Matrigel around the rim of the wells form a solid thin ring as depicted in 1 and photographed in 2, which has decreasing thickness. The picture in 3 acquired with a cell imager shows tumor organoids growing at the periphery of the well as desired, with no invasion of the center. (b) Proliferation of primary tumor cells as measured by ATP release. Different seeding densities were tested and compared (5, 10 and 15K cells). The mini-ring method allowed the patient sample to grow and maintain the heterogeneity and histology of the original ovarian tumor which had a high-grade serous carcinoma component (H&E left picture) and a clear cell component (H&E right picture). (c) Schematic of the drug-treatment experiments performed in the mini-ring setting. The pictures are representative images as acquired using a Celigo cell imager. (d - g) Assays to monitor drug response of cell lines using the mini-ring configuration. Three drugs (ReACp53, Staurosporine and Doxorubicin) were tested at five concentrations in triplicates for all cell lines. (d) ATP release assay (CellTiter-Glo 3D) readout. (e) and (f) Calcein/PI readout. (e) Representative image showing staining of MCF7 cells with the dyes and segmentation to quantify the different populations (live / dead). (f) Quantification of Calcein/PI assay for three-drug assay. (g) Quantification of cleaved caspase 3/7 assay. Doxorubicin was omitted due to its fluorescence overlapping with the caspase signal. For all graphs, symbols are individual replicates, bars represent the average and error bars show SD.

cence-based ATP assay to obtain a metabolic readout of cell status, calculate EC_{50} and identify cell-specific sensitivities (Fig. 1, S2 and S3). Results show how the Matrigel in the mini-ring setup is thin enough to allow penetration not only of small molecules but also of higher molecular weight biologics such as peptides[17]. We performed two consecutive treatments which allows the drugs to not only penetrate the gel but also to reach organoids that may be bulky[17]. However, the assay is flexible and can be easily adapted to single treatments followed by longer incubations, multiple consecutive recurring treatments, multi-drug combinations or other screening strategies (Fig. S3).

We also implemented assays to quantify drug response by measuring cell viability after staining of live organoids with specific dyes followed by imaging. A calcein-release assay coupled to propidium iodide (PI) staining as well as a caspase 3/7 cleavage assay can be readily performed after seeding the cells in standard black plates (Fig. 1e-g and S4). Tumor organoids are stained with the reagents after dispase release. After a 30-45 minute incubation, organoids can be imaged, followed by segmentation and quantification of the pictures (Fig. 1e-g and S4). All the assays described here are performed by measuring cell status in within the same well in which spheroids are seeded. Although the various assays we introduce are testing different aspects of cell viability and measure distinct biological events, results were mostly concordant across the methods for the three drugs tested (Fig. 1, S4).

Identification of actionable drug responses in PDTOs

A rapid functional assay to determine drug sensitivities of primary specimens can offer actionable information to help tailoring therapy to individual cancer patients[3]. We tested suitability of our approach to rapidly and effectively identify drug susceptibilities of three primary ovarian cancer samples and one high-grade serous peritoneal cancer specimen obtained from the operating room (Table S1; Fig. 2 and 3). In all cases, ascites or tumor samples were processed after surgery (see Methods) and then plated as mini-rings as described above. In order to maximize the amount of information

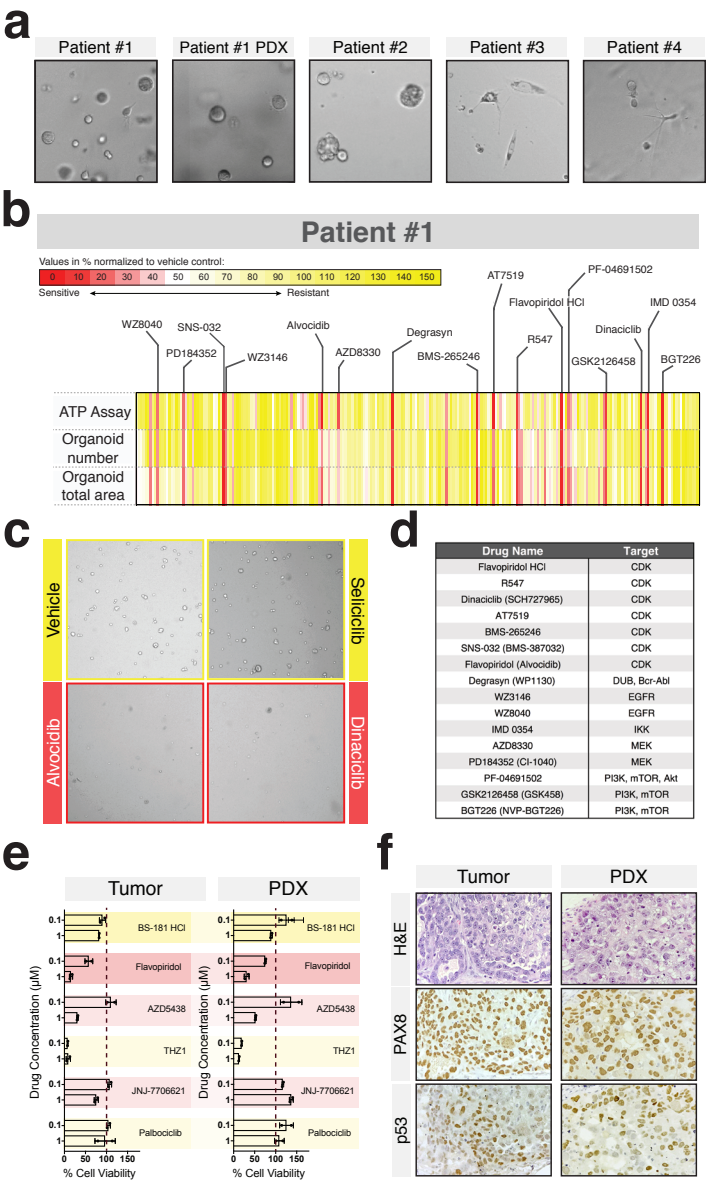

Drug Name	Target
Flavopiridol HCl	CDK
R547	CDK
Dinaciclib (SCH727965)	CDK
AT7519	CDK
BMS-265246	CDK
SNS-032 (BMS-387032)	CDK
Flavopiridol (Alvocidib)	CDK
Degrasyn (WP1130)	DUB, Bcr-Abl
WZ3146	EGFR
WZ8040	EGFR
IMD 0354	IKK
AZD8330	MEK
PD184352 (CI-1040)	MEK
PF-04691502	PI3K, mTOR, Akt
GSK2126458 (GSK458)	PI3K, mTOR
BGT226 (NVP-BGT226)	PI3K, mTOR

Figure 2. Mini-ring approach to unveil drug response patterns in PDTOs. (a) Morphology of the PDTOs established in this study as visualized by brightfield microscopy. **(b)** Results of kinase screening experiment. Three readouts were used for this assay: ATP quantification as measured by CellTiter-Glo 3D and organoid number or size quantification evaluated by brightfield imaging. Brightfield images were segmented and quantified using the Celigo S Imaging Cell Cytometer Software. Both organoid number as well as total area were evaluated for their ability to capture response to drugs. In this plot, each vertical line is one drug, all 252 tested are shown. Values are normalized to the respective vehicle controls for

each method and expressed as %. **(c)** A representative image of the effects of the indicated drug treatments as visualized by the Celigo cell imager. **(d)** Table of drug leads causing ~75% cell death. **(e)** Small scale kinase assay on Patient #1 primary cells and PDX-derived cells. ATP readout. Four molecules not present in the high-content screening were tested. We included two previously tested drugs, Flavopiridol and BS-181 HCl, as positive and negative control respectively. **(f)** Comparison of the original tumor with the established PDX.

extracted from irreplaceable clinical samples, we investigated the possibility to concurrently perform multiple assays on the same plate. To do so, we first optimized the initial seeding cell number (5000 cells/well) to couple an ATP metabolic assay to 3D tumor count and total organoid area measurement. This seeding density yields a low-enough number of organoids to facilitate size distribution analysis but sufficient ATP signal to be within the dynamic range of the CaspaseGlo 3D assay. For each patient sample, we seeded six 96 well plates and tested 252 different kinase inhibitors at two different concentrations (120 nM and 1 μM). We used the same experimental paradigm optimized above. All steps (media change, drug treatment) were automat-

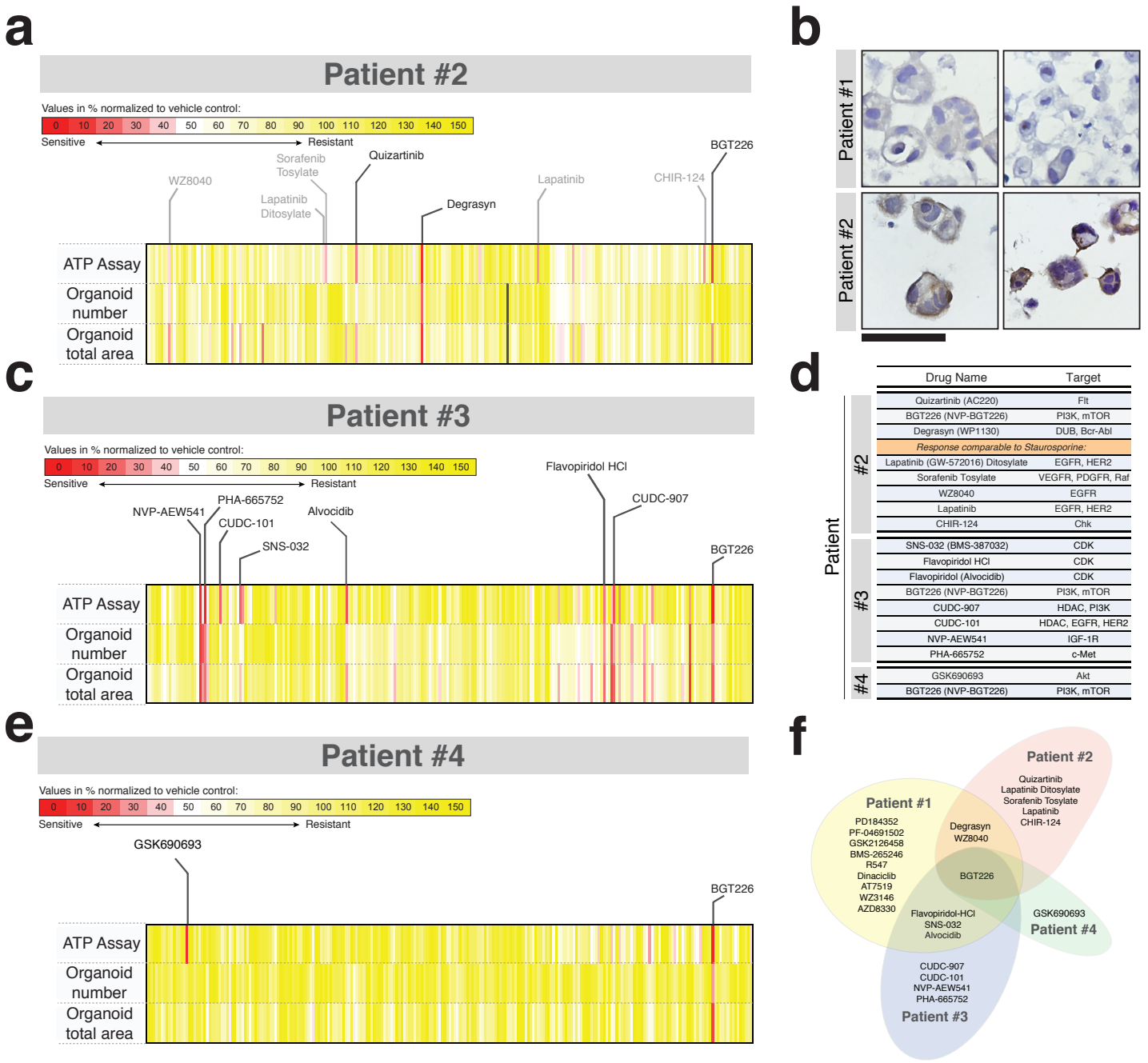

	Drug Name	Target
Patient #2	Quizartinib (AC220)	Flt
	BGT226 (NVP-BGT226)	PI3K, mTOR
	Degrasyn (WP1130)	DUB, Bcr-Abl
	Response comparable to Staurosporine:	
	Lapatinib (GW-572016) Ditosylate	EGFR, HER2
	Sorafenib Tosylate	VEGFR, PDGFR, Raf
	WZ8040	EGFR
	Lapatinib	EGFR, HER2
	CHIR-124	Chk
Patient #3	SNS-032 (BMS-387032)	CDK
	Flavopiridol HCl	CDK
	Flavopiridol (Alvocidib)	CDK
	BGT226 (NVP-BGT226)	PI3K, mTOR
	CUDC-907	HDAC, PI3K
	CUDC-101	HDAC, EGFR, HER2
	NVP-AEW541	IGF-1R
	PHA-665752	c-Met
Patient #4	GSK690693	Akt
	BGT226 (NVP-BGT226)	PI3K, mTOR

Figure 3. Individualized response of PDTOs to tyrosine kinase inhibitors. (a), (c) and **(e)** Results of kinase screening experiment on Patients 2-4 organoids. Each vertical line represents one of 252 tested drugs. Values are normalized to the respective vehicle controls (DMSO) for each method and expressed as %. **(b)** Expression of the multi-drug efflux protein ABCB1 in PDTOs as visualized by IHC. Patient #2 expresses very high levels of the ABC transporter. Scale bar: 60 μm. **(d)** Table of drug leads causing ~75% cell death. For Patient #2, we included drugs inducing a response comparable to the Staurosporine control (~60% cell death). **(f)** Diagram illustrating limited overlap between the detected patterns of response identified through the mini-ring assay for all patients.

ed and performed in less than 2 minutes/plate using a Beckman Coulter Biomek FX integrated into a Thermo Spinnaker robotic system. At the end of each experiment, PDTOs are first imaged in brightfield mode for organoid count/size distribution analysis followed by the ATP assay. The measurements yielded high quality data that converged on several hits, highlighting the feasibility of our approach to identify potential leads (Fig. 2 and 3).

Cells obtained from Patient #1 at the time of cytoreductive surgery[26] were chemo-naïve, and the heterogeneous nature of this clear cell/HGSC tumor was recapitulated in the PDTOs (Table 1 and Fig. 1b). The organoids were sensitive to 16/252 molecules tested and responded mostly to a variety of cyclin-dependent kinase (CDK) inhibitors with a stronger response to inhibitors hitting CDK1/2 in combination with CDK 4/6 or CDK 5/9 (Fig. 2b-d and S5a-b). Interestingly, CDK inhibitors have found limited applicability in ovarian cancer therapy so far[27]. Based on the profiles of the CDK inhibitors tested and on the response observed (Fig. S5a-b), we selected four untested molecules to assay. We anticipated that Patient #1 would not respond to Palbociclib (targeting only CDK4/6) and THZ1 (CDK7) while expecting a response to JNJ-7706621 (CDK1/2/3/4/6) and AZD54338 (CDK1/2/9; Fig. S5a-b). However, we observed a strong response to THZ1 (Fig. 2e). Both THZ1 and BS-181 HCl specifically target CDK7. Nevertheless, Patient #1 PDTOs showed a strong response to the former but no response to the latter which could be attributed to the different activity of the two as recently observed in breast cancer[28]. We also attempted to establish patient-derived xenografts (PDX) in vivo by injecting Patient #1 cells injected in NSG mice (500K/mouse, 12 mice). Only three mice developed PDXs over the course of several months, with xenografts closely resembling the original tumors (Fig. 2f). Organoids established from one of Patient #1 PDXs qualitatively recapitulated the response to CDK inhibitors, confirming that our strategy can be successfully used to test patient samples that are recalcitrant to grow in vivo, reducing time and costs (Fig. 2e).

Patient #2 was diagnosed with progressive, platinum-resistant HGSC and was heavily pretreated prior to sample procurement (Table S1). Patient #2 PDTOs showed a strong response to only 3/252 drugs tested (Fig. 3a and S5c). Moderate responses (50-60% residual cell viability at 1 μM) were observed for EGFR inhibitors and we could detect high expression of EGFR at the plasma membrane of the tumor cells (Fig. 3a, 3d and S5f). Remarkably, Patient #2 PDTOs showed a very moderate response to our positive control, Staurosporine, a pan-kinase inhibitor with very broad activity[29]. The significant lack of response to multiple therapies observed for Patient #2 led us to hypothesize that there could be over-expression of efflux membrane proteins. Indeed, the PDTOs showed a high level of expression of ABCB1 (Fig. 3b). High expression of the ATP-dependent detox protein ABCB1 is frequently found in chemoresistant ovarian cancer cells and recurrent ovarian cancer patients' samples and has been correlated with poor prognosis[30,31].

Patient #3 presented with carcinosarcoma of the ovary, an extremely rare and aggressive ovarian tumor which has not been fully characterized at the molecular level yet[32] (Table 1, Fig. 3c, 3d and Fig. S5d). In our screening, this tumor responded to 8/252 drugs, including CDK inhibitors and histone deacetylase inhibitors (HDACi). HDACi have been shown to reduce spheroid formation and restore epithelial differentiation in ovarian cancer models[33]. Patient #4 was diagnosed with a high-grade peritoneal tumor and responded to only 2/252 drugs, one Akt inhibitor (GSK690693) and a PI3K/mTOR inhibitor (BGT226; Table 1, Fig. 3d, 3e and Fig. S5e). Overall, there was very little overlap in the response observed from the four clinical samples, with the exception of BGT226 which showed activity in all tumors (Fig. 3f). A Phase I basket trial of this PI3K/mTOR inhibitor highlighted moderate responses in unstratified patients[34]. Overall, patient with or without PI3K alterations have been shown to respond to PI3K inhibitors[34]. Our assay could supersede the lack of predictors of response to PI3K inhibitors, and identify responsive tumors from a functional standpoint.

Conclusions

We devised and optimized a facile high-throughput approach to establish and screen tumor organoids. While we applied the mini-ring setup to drug screenings, the same methodology is suitable for studies aiming at characterizing organoids' biological and functional properties with medium to high throughput. Complete automation, scalability to 384 well plates, and flexibility to use different supports beside Matrigel can further extend the applicability of our mini-ring approach. Our methodology can be a robust tool to standardize functional precision medicine efforts[3], given its ease of applicability to many different systems and drug screening protocols, as well as its limited cell requirement which allows testing of samples as obtained from biopsies/surgical specimens without the need for expansion in vitro or in vivo which can lead to substantial divergence from the tumor of origin[35].

As demonstrated above, the method rapidly allowed us to pinpoint individual drug sensitivities and identify a tumor "fingerprint", with multiple inhibitors converging on a given pathway. Interestingly, many of the drugs identified in our screening do not have a specific, unequivocal biomarker or genomic signature predictive

of response. Thus, patients may greatly benefit from PDTO testing prior to therapy selection, either to identify a suitable therapy or to facilitate patient selection for clinical trials[3,4,13,15,36].

Acknowledgments

This project was supported by a Worldwide Cancer Research grant to AS (#16-0253). We acknowledge support by the Hirshberg Foundation (to AS), the UCLA SPORE in Prostate Cancer (NIH P50CA092131, PI: Robert Reiter) and a Jonsson Cancer Center Foundation Impact Award (to SM).

Author Contributions

AS and NP designed the project and carried out the experiments. JJH and MM performed experiments on clinical samples. SM obtained the patient samples. JH contributed to feasibility experiments. BT and RB generated the kinase inhibitor drug library and optimized automation for primary sample assays. AS analyzed the data and wrote the paper with contributions from all authors.

References

1. Cummings, C., Peters, E., Lacroix, L., Andre, F. & Lackner, M. The Role of Next-Generation Sequencing in Enabling Personalized Oncology Therapy. Clinical And Translational Science 9, 283–292 (2016).
2. Simon, R. & Roychowdhury, S. Implementing personalized cancer genomics in clinical trials. Nature Reviews Drug Discovery 12, nrd3979 (2013).
3. Letai, A. Functional precision cancer medicine—moving beyond pure genomics. Nat Med 23, 1028–1035 (2017).
4. Vlachogiannis, G. et al. Patient-derived organoids model treatment response of metastatic gastrointestinal cancers. Science 359, 920–926 (2018).
5. Voest, E. E. & Bernards, R. DNA-Guided Precision Medicine for Cancer: A Case of Irrational Exuberance? Cancer Discov 6, 130–132 (2016).
6. Prasad, V., Fojo, T. & Brada, M. Precision oncology: origins, optimism, and potential. Lancet Oncol. 17, e81–e86 (2016).
7. Tannock, I. F. & Hickman, J. A. Limits to Personalized Cancer Medicine. New England Journal of Medicine 375, 1289–1294 (2016).
8. Leitao, M. M. et al. Mutation and expression of the TP53 gene in early stage epithelial ovarian carcinoma. Gynecol. Oncol. 93, 301–306 (2004).
9. Pickl, M. & Ries, C. H. Comparison of 3D and 2D tumor models reveals enhanced HER2 activation in 3D associated with an increased response to trastuzumab. Oncogene 28, 461–468 (2008).
10. Katt, M. E., Placone, A. L., Wong, A. D., Xu, Z. S. & Searson, P. C. In Vitro Tumor Models: Advantages, Disadvantages, Variables, and Selecting the Right Platform. Front Bioeng Biotechnol 4, (2016).
11. Tanner, K. & Gottesman, M. M. Beyond 3D culture models of cancer. Sci Transl Med 7, 283ps9 (2015).
12. Nyga, A., Cheema, U. & Loizidou, M. 3D tumour models: novel in vitro approaches to cancer studies. J Cell Commun Signal 5, 239–248 (2011).
13. Fong, S., Debs, R. J. & Desprez, P.-Y. Id genes and proteins as promising targets in cancer therapy. Trends in Molecular Medicine 10, 387–392 (2004).
14. Kimlin, L. C., Casagrande, G. & Virador, V. M. In vitro three-dimensional (3D) models in cancer research: an update. Mol. Carcinog. 52, 167–182 (2013).
15. Pauli, C. et al. Personalized In Vitro and In Vivo Cancer Models to Guide Precision Medicine. Cancer Discov 7, 462–477 (2017).
16. Halfter, K. & Mayer, B. Bringing 3D tumor models to the clinic - predictive value for personalized medicine. Biotechnol J 12, (2017).
17. Soragni, A. et al. A Designed Inhibitor of p53 Aggregation Rescues p53 Tumor Suppression in Ovarian Carcinomas. Cancer Cell 29, 90–103 (2016).
18. Breslin, S. & O'Driscoll, L. Three-dimensional cell culture: the missing link in drug discovery. Drug Discovery Today 18, 240–249 (2013).
19. Breslin, S. & O'Driscoll, L. The relevance of using 3D cell cultures, in addition to 2D monolayer cultures, when evaluating breast cancer drug sensitivity and resistance. Oncotarget 7, 45745–45756 (2016).
20. Friedrich, J., Seidel, C., Ebner, R. & Kunz-Schughart, L. A. Spheroid-based drug screen: considerations and practical approach. Nat Protoc 4, 309–324 (2009).
21. Zanoni, M. et al. 3D tumor spheroid models for in vitro therapeutic screening: a systematic approach to enhance the biological relevance of data obtained. Sci Rep 6, 19103 (2016).
22. Kelm, J. M., Timmins, N. E., Brown, C. J., Fussenegger, M. & Nielsen, L. K. Method for generation of homogeneous multicellular tumor spheroids applicable to a wide variety of cell types. Biotechnol. Bioeng. 83, 173–180 (2003).
23. Boj, S. F. et al. Organoid models of human and mouse ductal pancreatic cancer. Cell 160, 324–338 (2015).
24. Walsh, A. J. et al. Quantitative optical imaging of primary tumor organoid metabolism predicts drug response in breast cancer. Cancer Res. 74, 5184–5194 (2014).
25. Francies, H. E., Barthorpe, A., McLaren-Douglas, A., Barendt, W. J. & Garnett, M. J. Drug Sensitivity Assays of Human Cancer Organoid Cultures. Methods Mol. Biol. (2016). doi:10.1007/7651_2016_10
26. Janzen, D. M. et al. An apoptosis-enhancing drug overcomes platinum resistance in a tumour-initiating subpopulation of ovarian cancer. Nat Commun 6,

(2015).
27. Zhou, Q. Targeting Cyclin-Dependent Kinases in Ovarian Cancer. Cancer Investigation 0, 1–10 (2017).
28. Li, B. et al. Therapeutic Rationale to Target Highly Expressed Cdk7 Conferring Poor Outcomes in Triple-Negative Breast Cancer. Cancer Res canres.2546.2016 (2017). doi:10.1158/0008-5472.CAN-16-2546
29. Belmokhtar, C. A., Hillion, J. & Ségal-Bendirdjian, E. Staurosporine induces apoptosis through both caspase-dependent and caspase-independent mechanisms. Oncogene 20, 3354–3362 (2001).
30. Sun, S. et al. Prognostic Value and Implication for Chemotherapy Treatment of ABCB1 in Epithelial Ovarian Cancer: A Meta-Analysis. PLoS One 11, (2016).
31. Vaidyanathan, A. et al. ABCB1 (MDR1) induction defines a common resistance mechanism in paclitaxel- and olaparib-resistant ovarian cancer cells. Br J Cancer 115, 431–441 (2016).
32. Rauh-Hain, J. A., Birrer, M. & Del Carmen, M. G. Carcinosarcoma of the ovary, fallopian tube, and peritoneum: Prognostic factors and treatment modalities. Gynecol. Oncol. 142, 248–254 (2016).
33. Tang, H. M. et al. An epithelial marker promoter induction screen identifies histone deacetylase inhibitors to restore epithelial differentiation and abolishes anchorage independence growth in cancers. Cell Death Discovery 2, 16041 (2016).
34. Markman, B. et al. Phase I safety, pharmacokinetic, and pharmacodynamic study of the oral phosphatidylinositol-3-kinase and mTOR inhibitor BGT226 in patients with advanced solid tumors. Ann Oncol 23, 2399–2408 (2012).
35. Ben-David, U. et al. Patient-derived xenografts undergo mouse-specific tumor evolution. Nature Genetics 49, 1567–1575 (2017).
36. Huang, L. et al. Ductal pancreatic cancer modeling and drug screening using human pluripotent stem cell- and patient-derived tumor organoids. Nat. Med. 21, 1364–1371 (2015).

Methods

Cell lines and primary samples: Cell lines are cultured in their recommended medium in the presence of 10% FBS (Life Technologies #10082-147) and 1% Antibiotic-Antimycotic (Gibco). DU145, PC3, PANC1 and HUTP4 were culture in DMEM (Life Technologies #1195-065). PAN03.27, MDA-MB-468 and MCF-7 was cultured in RPMI (Life Technologies #22400-089). SK-NEP-1 was cultured in McCoy medium (ATCC #30-2007). S9 GODL cells are derived from HGSOC primary samples and cultured in RPMI. All treatments are performed in serum-free medium (PrEGM, Lonza #CC-3166, MammoCult, StemCell Technologies # 05620).
Primary samples: Primary ovarian cancer specimens were dissociated to single cells and cryopreserved or plated right after processing. In short, fresh tumor specimens or ascites samples are obtained from consented patients (UCLA IRB 10-000727). Solid tumor specimens are minced, then enzymatically digested with collagenase IV (200 U/ml). The resulting cell suspension is filtered through a 40 µM cell strainer.

Chemicals: Doxorubicin hydrochloride was purchased from Sigma (#44583). Staurosporine was purchased from Cell Signaling Technology (#9953S). ReACp53 was synthesized by GL Biochem and prepared as described in Soragni et al, 2016.

3D organoids seeding/treatment procedure: Single-cell suspensions (2K-10K/well) were plated around the rim of the well of 96 well plates in a 3:4 mixture of PrEGM medium and Matrigel (BD Bioscience CB-40324). White plates (Corning #3610) were used for ATP assays while black ones (Corning #3603) were used for caspase or calcein assays. Plates are incubated at 37°C with 5% CO2 for 15 minutes to solidify the gel before addition of 100 μl of pre-warmed PrEGM to each well using an EpMotion (Eppendorf). Two days after seeding, medium is removed and replaced with fresh PrEGM containing the indicated drugs. The same procedure is repeated daily on two consecutive days. 24h after the last treatments, media is removed and wells are washed with 100 μl of pre-warmed PBS. To prepare for downstream experiments, organoids are then released from Matrigel by 40 minutes of incubation in 50 μl of 5mg/mL dispase (Life Technologies #17105-041). All steps are performed with the EpMotion for small scale experiments and medium is removed/added from the center of the wells. For the high-throughput kinase screening experiment, we utilized a Beckman Coulter Biomek FX system with 96 channel head integrated into a Thermo Spinnaker robotic system with Momentum scheduling software. In short, an intermediary dilution plate (Axygen P-96-450V-C-S) was filled with 100 μl/well of media and pre-warmed to 37°C. Using pre-sterilized p50 tips, 1 μl of drug is transferred from a library compound plate to the intermediary media plate and thoroughly mixed. Next, the robot gently removed 100 μl of media from the matrigel/cell plate. The liquid handler was set up to hit the dead center of each well with no contact to the Matrigel mini-ring. As a last step, the robot transferred 100 μl from the intermediary plate (media+drug) to the matrigel/cell plate. Media was easily dispensed without touching or disrupting the Matrigel mini-ring. The total process time outside of the CO2 incubator was less than 2 minutes allowing the temperature to be controlled throughout.

ATP assay: After the organoid release, 75 μl of Celltiter-Glo 3D Reagent (Promega #G968B) is added to

each well followed by 1 minute of vigorous shaking. After a 30 minute incubation at room temperature and an additional minute of shaking, luminescence is measured with a SpectraMax iD3 (Molecular Devices) over 500 ms of integration time. Data is normalized to vehicle and plotted and EC50 values are calculated with Prism 7. For the high-throughput drug screening, DMSO and Staurosporine (1 μM) are used as negative and positive control respectively. Values are normalized to vehicle. Hits are determined following two criteria: (1) cell death shows concentration-dependency and (2) residual cell viability at 1 μM is ≤ 25%. For Patient #2, partial hits are defined as drugs giving response comparable to Staurosporine (50-60% residual viability at 1 μM).

Caspase 3/7/Hoechst assay: After dispase treatment, 100 μl of Nexcelom ViaStain™ Live Caspase 3/7 staining solution is added to each well. The staining solution consists of 2.5 μM Caspase reagent (Nexcelom #CSK-V0002) and 3 μg/ml Hoechst (Nexcelom #CS1-0128) in serum-free RPMI medium. Plates are incubated 37°C/5% CO2 for 45 minutes and imaged with a Celigo S Imaging Cell Cytometer (Nexcelom). Data is normalized to vehicle values and plotted with Prism 7.

Calcein-AM/Hoechst/Viability assay: For this assay, 100 μl of Calcein-AM/Hoechst/PI viability staining solution are added to each well containing the released organoids. The staining solution includes the Calcein-AM reagent (Nexcelom CS1 #0119; 1:2000 dilution), Propidium Iodide (Nexcelom #CS1-0116; 1:500 dilution), Hoechst (Nexcelom #CS1-0126; 1:2500 dilution) in serum-free RPMI medium. Samples are incubated for 15 minutes at 37°C with 5% CO2 before imaging with a Celigo S Imaging Cell Cytometer (Nexcelom).

Immunohistochemistry: Cells processed for fixation were seeded in 24 well plates to facilitate collection. Rings are washed with pre-warmed PBS, followed by 30-minute fixation at room temperature with 4% Formaldehyde EM-Grade (Electron Microscopy Science #15710). Samples are collected in a conical tube and centrifuged at 2000g for 10 minutes at 4oC. Pellets are washed with PBS followed by a second spin. After discarding the supernatant, pellets are mixed in 10 μl of HistoGel (ThermoScientific #HG-40000-012). The mixture is shortly incubated on ice for 5 minutes to solidify the pellets before transferring to a histology cassette for standard embedding and sectioning.

The slides are baked at 45oC for 20 minutes and de-paraffinized in xylene followed by washes in ethanol and D.I. water. Endogenous peroxidases are blocked with Peroxidazed-1 (Biocare Medical #PX968M) at RT for 5 minutes. Antigen retrieval is performed in a NxGEN Deloaking Chamber (Biocare Medical) using Diva Decloacker (Biocare Medical #DV2004LX) at 110oC for 15 minutes for Ki-67/Caspase-3, PAX8 and p53 (Biocare Medical #PPM240DSAA) staining or using Borg Decloacker (Biocare Medical #BD1000 S-250) at 90oC for 15 minutes for Anti-P Glycoprotein (Abcam #EPR10364-57) staining. For EGFR staining, antigen retrieval is perfomed enzymatically with Carezyme III Pronase (Biocare Medical #PRT957) at 37oC for 5 minutes.

Blocking is performed at RT for 30 minutes with Background Punisher (Biocare Medical #BP947H) at RT for 15 minutes for the EGFR staining. Primary antibodies are diluted in Da Vinci Green Diluent (Biocare Medical #PD900L) for Anti-P Glycoprotein (1:300), p53 (1:200, Biocare Medical #CME298A) and PAX8 (1:1000, Proteintech #10336-1-A) incubated at 4oC overnight or Van Gogh Diluent (Biocare #PD902H) for EGFR (1:30) incubated at RT for 30 minutes. The combo Ki-67/Caspase-3 solution is pre-diluted and added to the sample for 60 minutes at room temperature. Secondary antibody staining is performed with Rabbit on Rodent HRP-polymer (Biocare Medical #RMR622G) for the Anti-P Glycoprotein, p53 and PAX8 staining or with Mouse on Mouse HRP-polymer (Biocare Medical #MM620G) for EGFR. MACH 2 double Stain 2 (Biocare Medical #MRCT525G) is used for Ki-67/Caspase-3 combinatorial staining. All secondary antibodies are incubated at RT for 30 minutes.

Chromogen development is performed with Betazoid DAB kit (Biocare Medical #BDB2004) for Anti-P Glycoprotein, pTEN and EGFR and Ki-67 or Warp Red Chromogen Kit (Biocare Medical #WR806) for Caspase-3. The reaction is quenched by dipping the slides in D.I water. Hematoxylin-1 (Thermo Scientific #7221) is used for counterstaining. The slides are mounted with Permount (Fisher Scientific #SP15-100). Images are acquired with a Revolve Upright and Inverted Microscope System (Echo Laboratories).

SUPPLEMENTARY MATERIAL

A simple high-throughput approach to identify actionable drug responses in patient-derived tumor organoids

Nhan Phan, Jenny J. Hong, Bobby Tofig, Matthew Mapua, Jin Huang, Sanaz Memarzadeh, Robert Damoiseaux and Alice Soragni

Supplementary Table:

Table S1. Characteristics of samples included in this study.

Stable Lines:

Specimen	Tumor Classification	Base Medium
MCF7	Invasive breast ductal carcinoma	RPMI
MD-MBA-468	Breast adenocarcinoma	RPMI
PANC1	Pancreatic ductal adenocarcinoma	DMEM
PANC03.27	Pancreatic adenocarcinoma	RPMI
HUPT4	Pancreatic adenocarcinoma	DMEM
PC3	Prostatic adenocarcinoma	DMEM
DU145	Prostatic carcinoma	DMEM
SK-NEP-1	Ewing sarcoma	McCoy
S9 GODL	High grade serous ovarian carcinoma	RPMI

Clinical Specimens:

Specimen	Tumor Classification	Stage	Sample Type	Therapy
Patient #1	High-grade mixed type carcinoma with a high grade serous (40%) and a clear cell carcinoma (60%) component	IIC	Ascites	None
Patient #2	High grade serous ovarian carcinoma	IIIC	Ascites	Carboplatin / Taxol / Avastin
Patient #3	Carcinosarcoma of the ovary with heterologous component	IIIC	Tumor	Carboplatin / Taxol
Patient #4	High grade serous carcinoma, primary peritoneal carcinoma	IIIC	Tumor	None

Supplementary Figures:

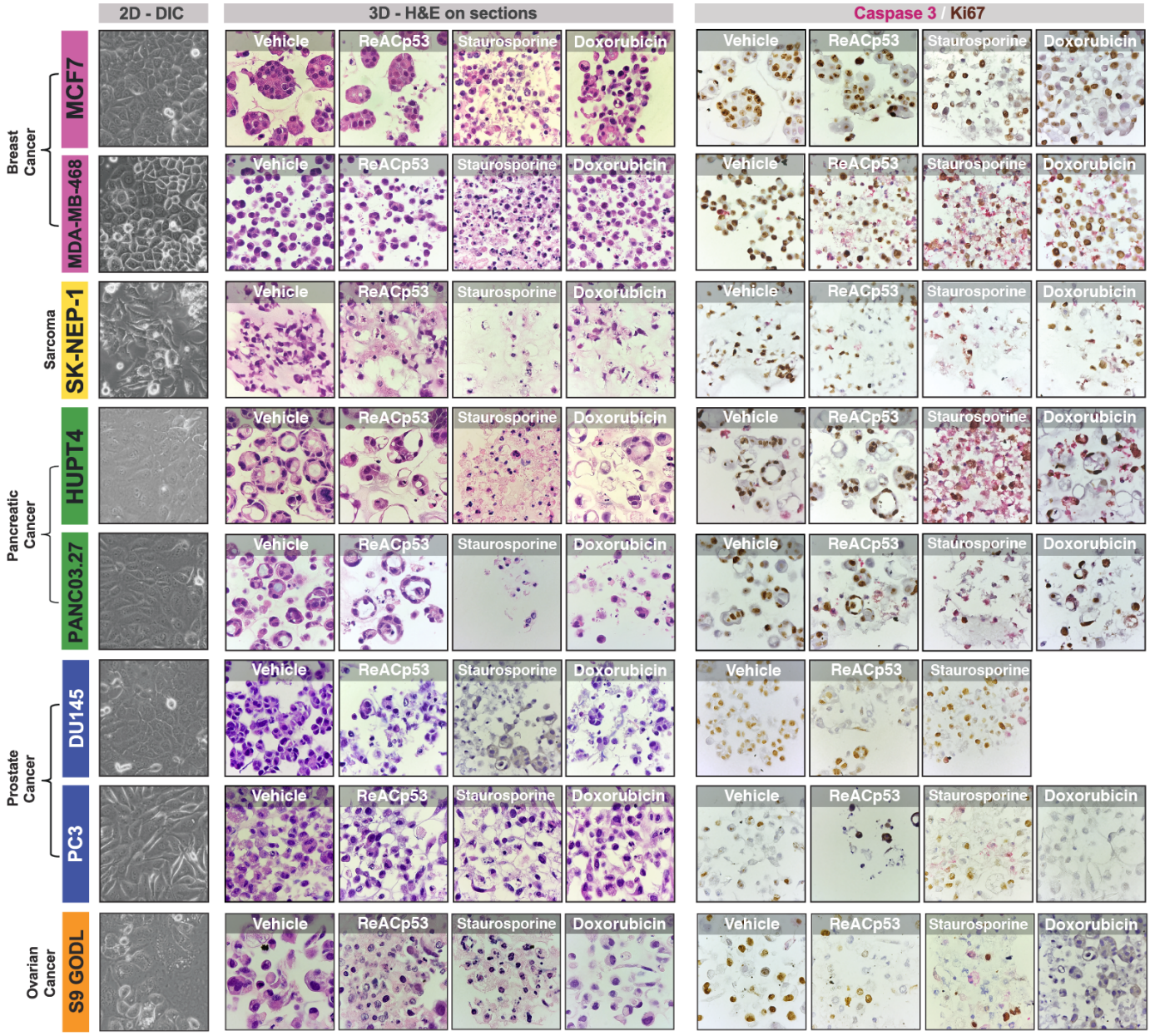

Figure S1. Morphology of 3D tumor models. Tumor cell lines used in this study grown in 3D processed for histology. The corresponding cells grown in 2D are shown on the left (40x magnification). On the right, H&E and Caspase/Ki67 staining on sections from embedded 3D tumor organoid samples (60x magnification).

a

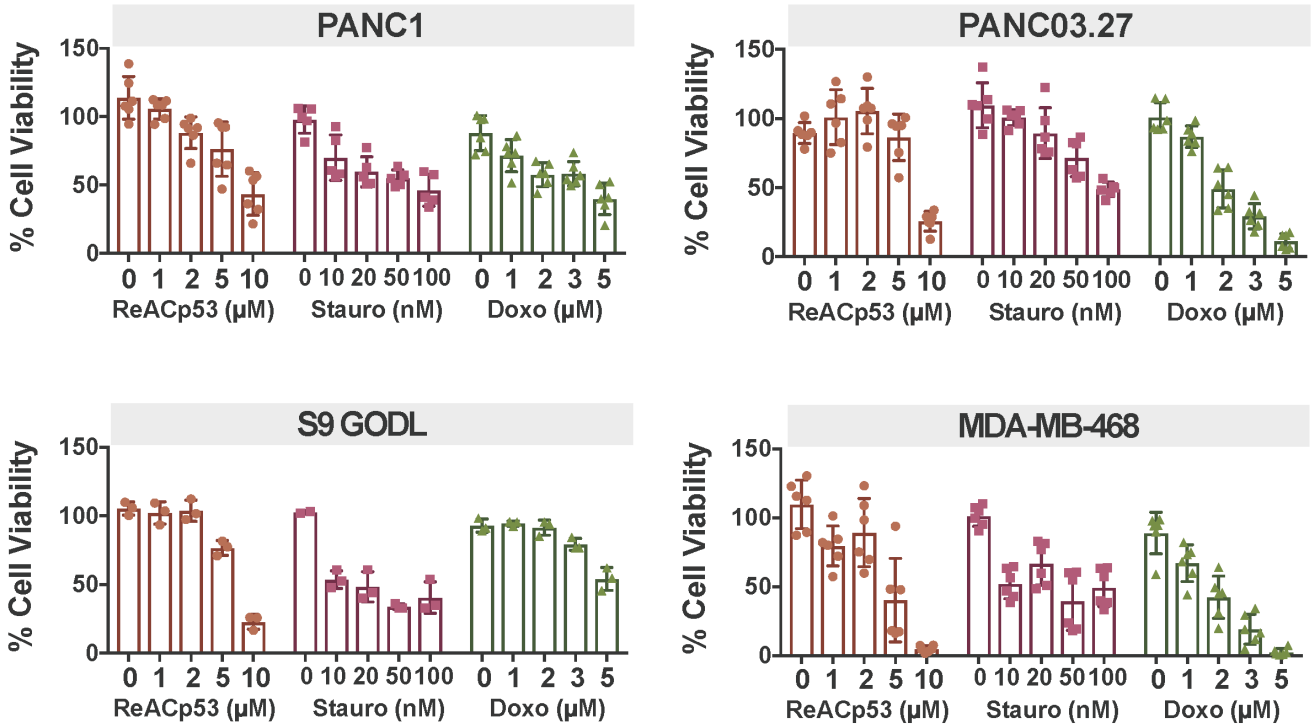

b

	ReACp53	Staurosporin	Doxorubicin
S9 GODL	7.5	0.2	5.9
SKNEP	2.9	0.3	0.9
MCF7	9.9	0.1	12.0
HUPT4	7.4	0.3	1.5
PANC1	6.9	ND	5.7
PANC03.27	8.5	0.8	2.1
MDA-MB-468	2.5	ND	1.7

Figure S2. ATP readout and EC_{50} values for three-drug assay. (a) ATP quantification as measured by CellTiter-Glo 3D. Data from 2 independent experiments, n=3 for each are plotted. Error bars represent standard deviation; bars represent mean values. **(b)** EC_{50} values as calculate from the ATP quantification data. All values are expressed in μM.

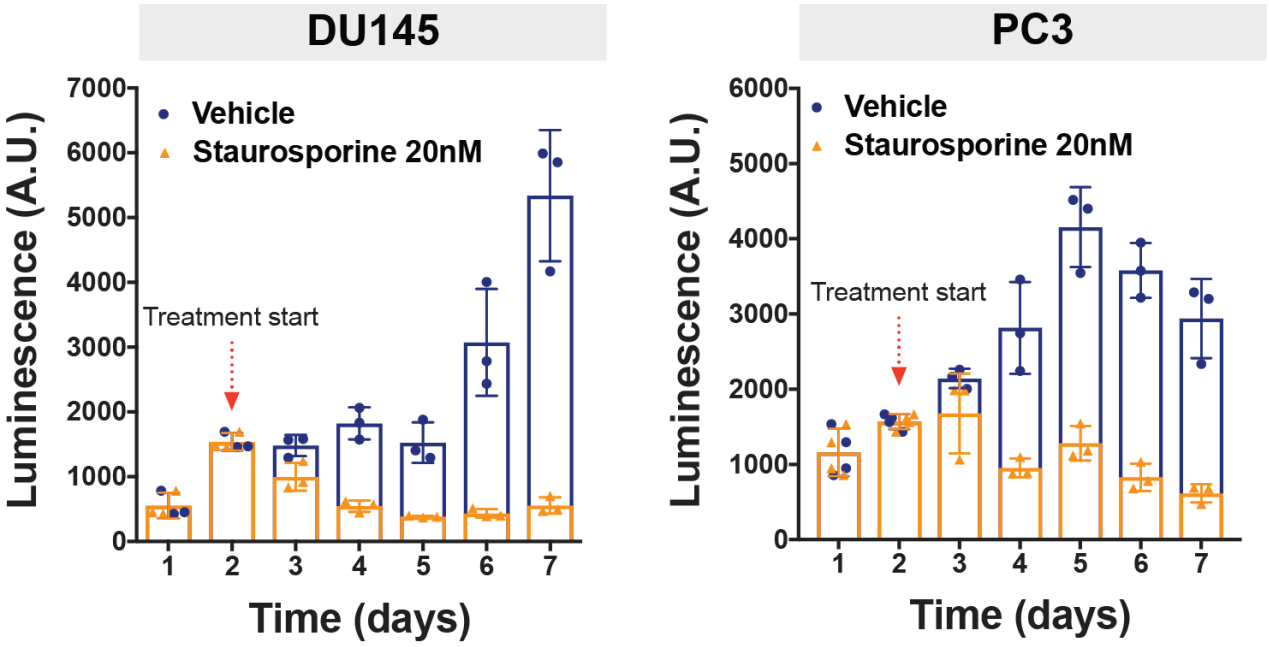

Figure S3. Adaptability of miniring assay to different treatment schedules. ATP quantification as measured by CellTiter-Glo 3D of prostate cancer organoids treated for 5 consecutive days with either vehicle or 20 nM Staurosporine.

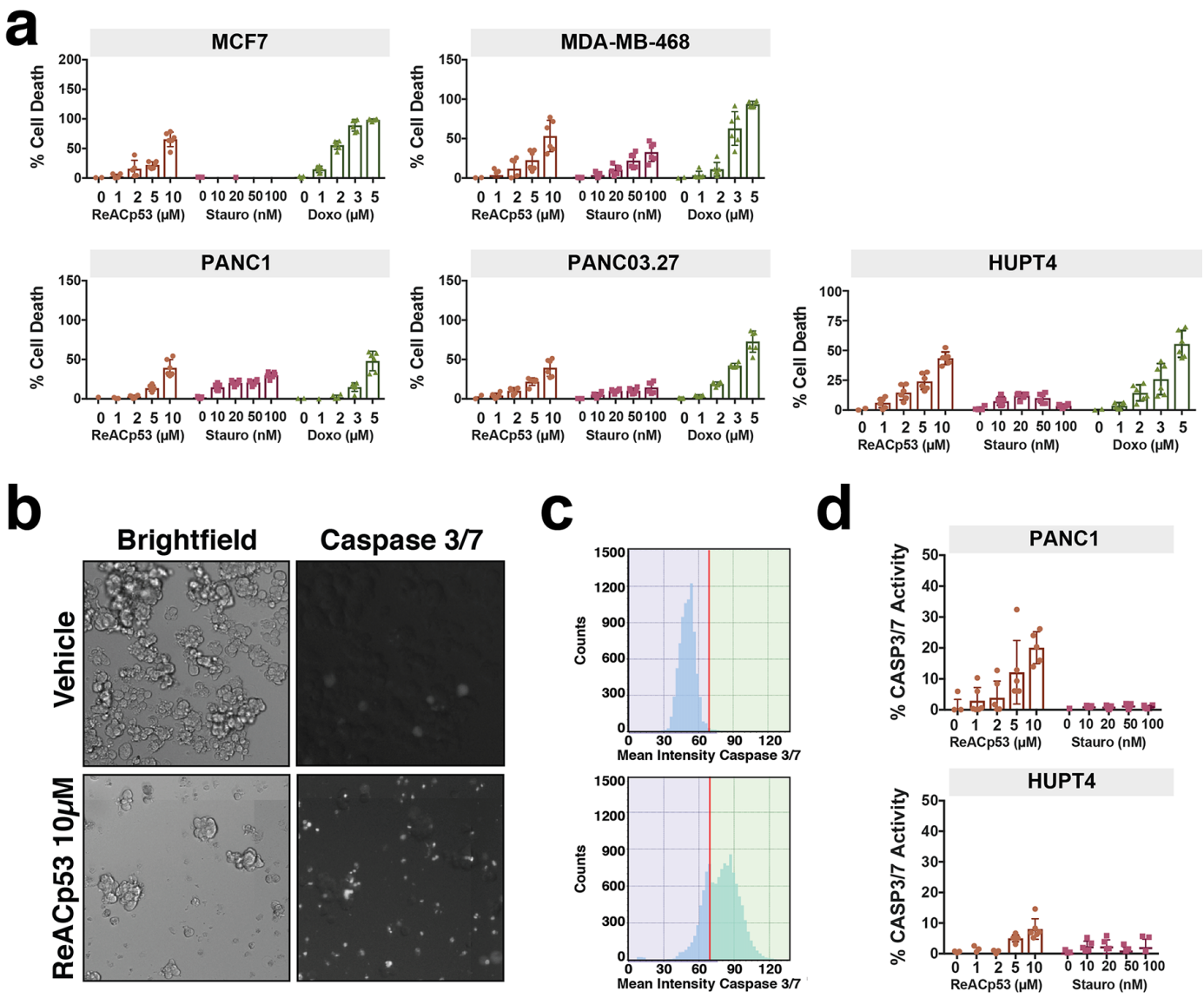

Figure S4. Additional optimized readouts for miniring assay (a) Quantification of the calcein release / PI uptake experiment. Two independent experiments shown, n=3 for each. Error bars are standard deviation while bars represent mean values. **(b)** and **(c)** Example of outcome for the caspase 3/7 cleavage experiment. DU145 prostate cancer cells are shown. A substrate becomes fluorescent when cleaved by caspase 3 or 7. Treatment induces high levels of caspase activation. Histograms of fluorescence intensity are shown in **(c)**. **(d)** Quantification of active caspase 3/7 activity normalized to control. Doxorubicin has intrinsic fluorescence that masks the caspase signal hence was excluded from this analysis.

a

Targets:	CDK1	CDK2	CDK3	CDK4	CDK5	CDK6	CDK7	CDK9	Other Targets
Flavopiridol (Alvocidib)	+++	+++		+++		+++	+		
R547	++++	++++		++++					GSK-3β
Dinaciclib (SCH727965)	++++	++++			++++			++++	
AT7519	++	++	+	++	+++	++	+	++++	GSK-3β
BMS-265246	++++	++++		++					
Flavopiridol (Alvocidib) HCl	+++	+++		+++		+++	+		
SNS-032 (BMS-387032)	+	+++		+	+		++	++++	GSK-3α,GSK-3β

b

Targets:	CDK1	CDK2	CDK3	CDK4	CDK5	CDK6	CDK7	CDK9	Other Targets
Roscovitine (Seliciclib,CYC202)		+			++				ERK2,GST-ERK1,ERK1
Milciclib (PHA-848125)	+	++		++	+		++		TrkA
PHA-793887	++	++++		++	++++		++++	++	GSK-3β
BS-181 HCl							+++		

c

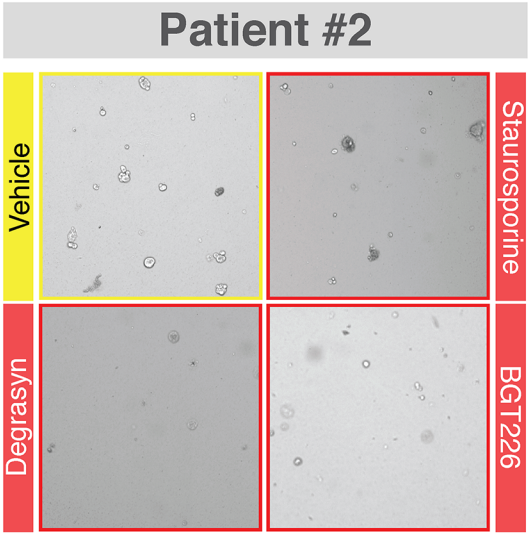

d

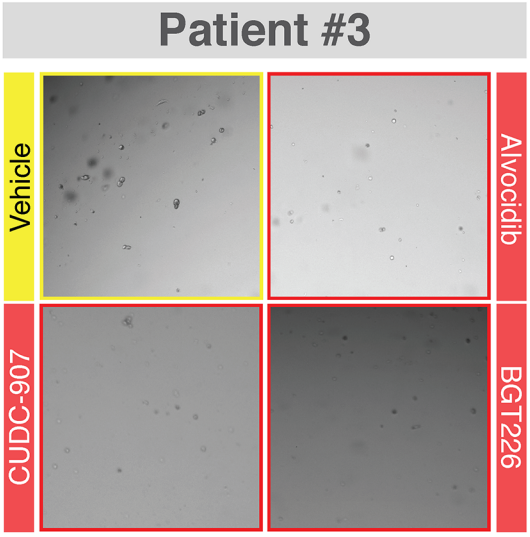

e

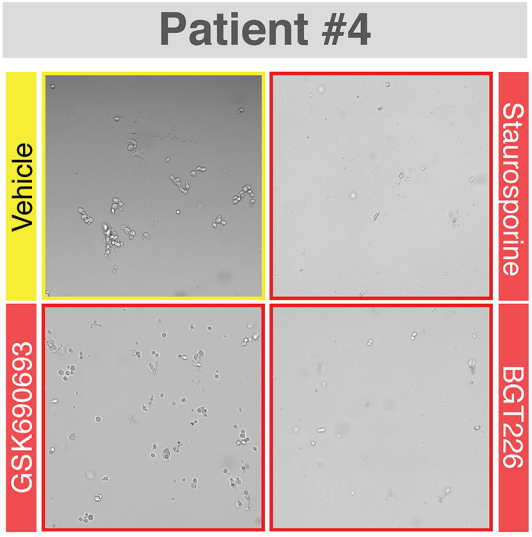

f

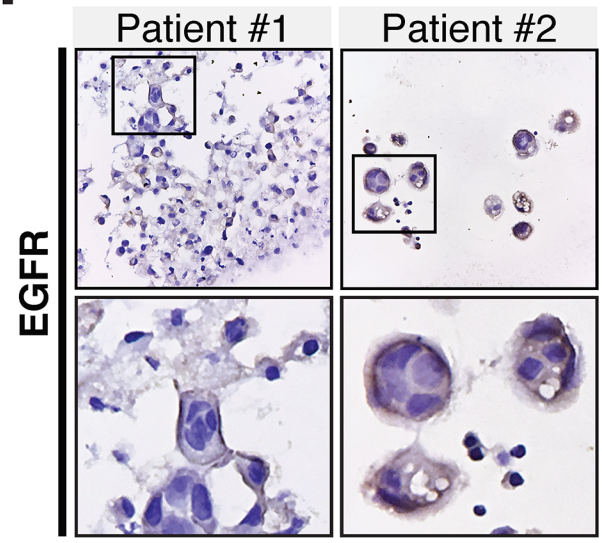

Figure S5. Results and validation of PDTO kinase screening. (a) Kinase inhibitors to which the HGSC control patient-derived line S1 GODL responded to. **(b)** List of CDK inhibitors that induced cell death in >75%Patient #1's organoids. Targets and specificity of each is listed. The patient responded to CDK inhibitors hitting CDK1/2 in combination with CDK 4/6 or CDK 5/9. **(c), (d) and (e)** Representative images of post-treatment and post-dispase PDTOs **(e)** Expression of EGFR in S1 GODL, Patient #1 and Patient #2 3D tumors. Magnification: 40x.